

# APPENDIX: Cyclical accretion regime change in the slow X-ray pulsar 4U 0114+65 observed with *Chandra*.

Sanjurjo-Ferrín, G.<sup>1</sup>, Torrejón, J.M.<sup>1</sup>, Postnov, K.<sup>2</sup>, Nowak, M.<sup>3</sup>, Rodes-Roca, J.J.<sup>1</sup>, Oskinova, L.<sup>4</sup>,  
Planelles-Villalva, J.<sup>1</sup>, Schulz, N.<sup>5</sup>,

<sup>1</sup>Instituto Universitario de Física Aplicada a las Ciencias y las Tecnologías, Universidad de Alicante, 03690 Alicante, Spain

<sup>2</sup>Sternberg Astronomical Institute, Moscow M.V. Lomonosov State University, Universitetskij pr, 13, Moscow 119234, Russia

<sup>3</sup>Department of Physics, Washington University in St. Louis, Missouri, USA

<sup>4</sup>Institute for Physics and Astronomy, Universität Potsdam, 14476 Potsdam, Germany

<sup>5</sup>MIT Kavli Institute for Astrophysics and Space Research, Cambridge, Massachusetts, USA

January 14, 2025

## ABSTRACT

4U 0114+65 is a high-mass X-ray binary system formed by the luminous supergiant B1Ia, known as V\* V662 Cas, and one of the slowest rotating neutron stars with a spin period of about 2.6 hours. This fact provides a rare opportunity to study interesting details of the accretion within each individual pulse of the compact object. In this paper, we analyze 200 ks of *Chandra* grating data, divided into 9 uninterrupted observations around the orbit. The changes in the circumstellar absorption column through the orbit suggest an orbital inclination of  $\sim 40^\circ$  with respect to the observer and a companion mass-loss rate of  $\sim 8.6 \cdot 10^{-7} M_\odot \text{ yr}^{-1}$ . The peaks of the NS pulse show a large pulse-to-pulse variability. Three of them show an evolution from a brighter regime to a weaker one. We propose that the efficiency of Compton cooling in this source fluctuates throughout an accumulation cycle. After significant depletion of matter within the magnetosphere, since the settling velocity is  $\sim \times 2$  times lower than the free-fall velocity, the source gradually accumulates matter until the density exceeds a critical threshold. This increase in density triggers a transition to a more efficient Compton cooling regime, leading to a higher mass accretion rate and consequently to an increased brightness.

## Appendix A: Light curves

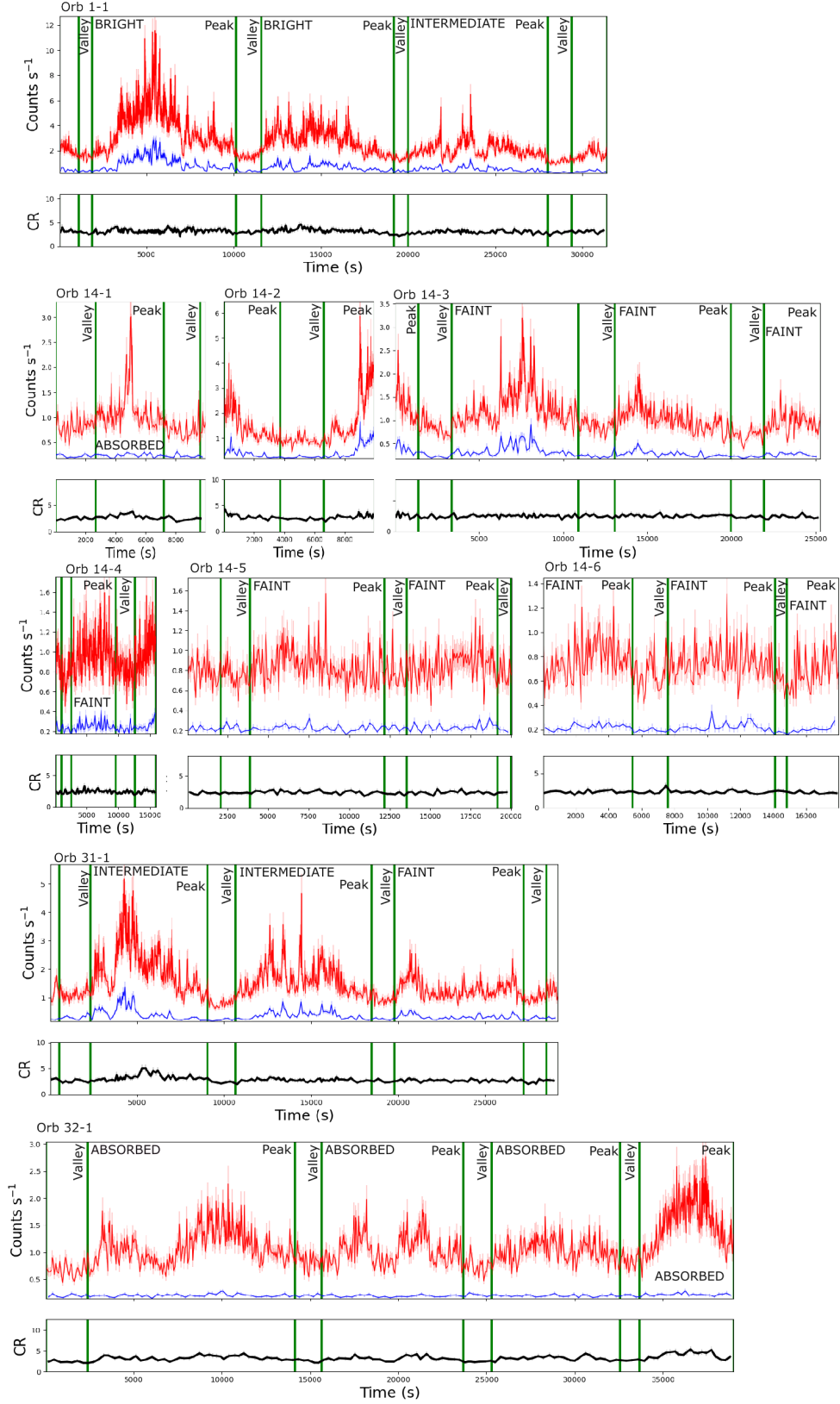


**Fig. A.1.** Concatenated light curves from the dataset, each labeled with its corresponding tag indicating the orbit and the sequential order within that orbit. For each light curve, the upper panel displays the high energy (3 – 10 keV, red) and low energy (0.3 – 3 keV, blue) light curves, while the lower panel shows their ratio (CR). Green vertical lines represent the boundaries for the peaks and valleys.

## Appendix B: Spectra

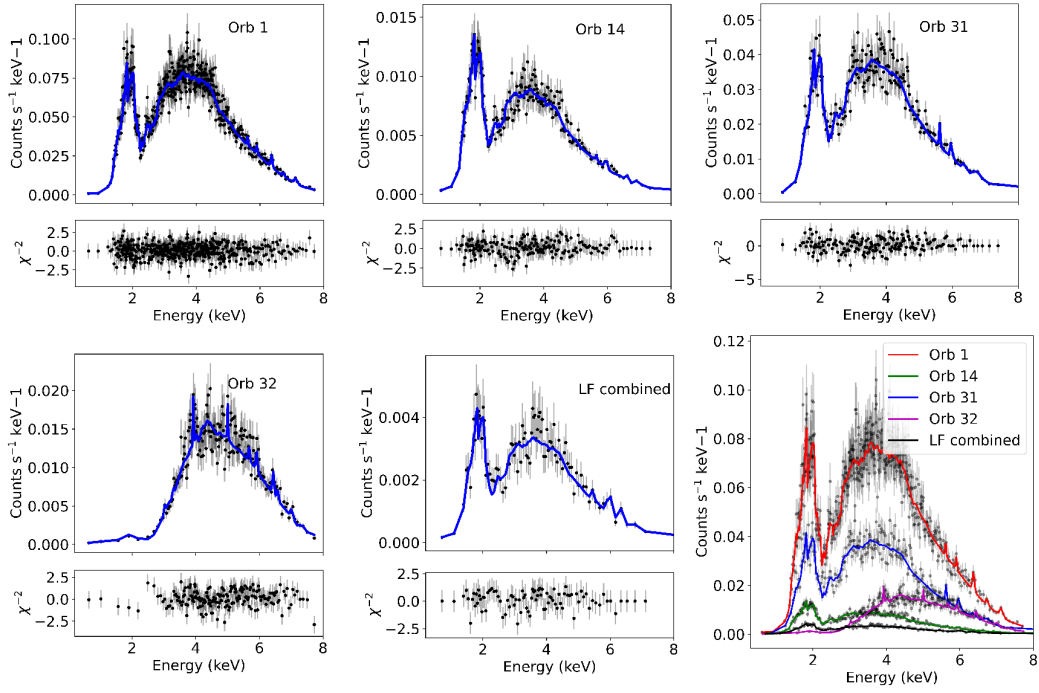


**Fig. B.1.** Upper row (left to right): Spectra, model, and  $\chi^2$  values for Orb 1, Orb 14, and Orb 31. Lower row (left to right): Spectra, model, and  $\chi^2$  values for Orb 32, valley combined, and all spectra displayed for comparison.

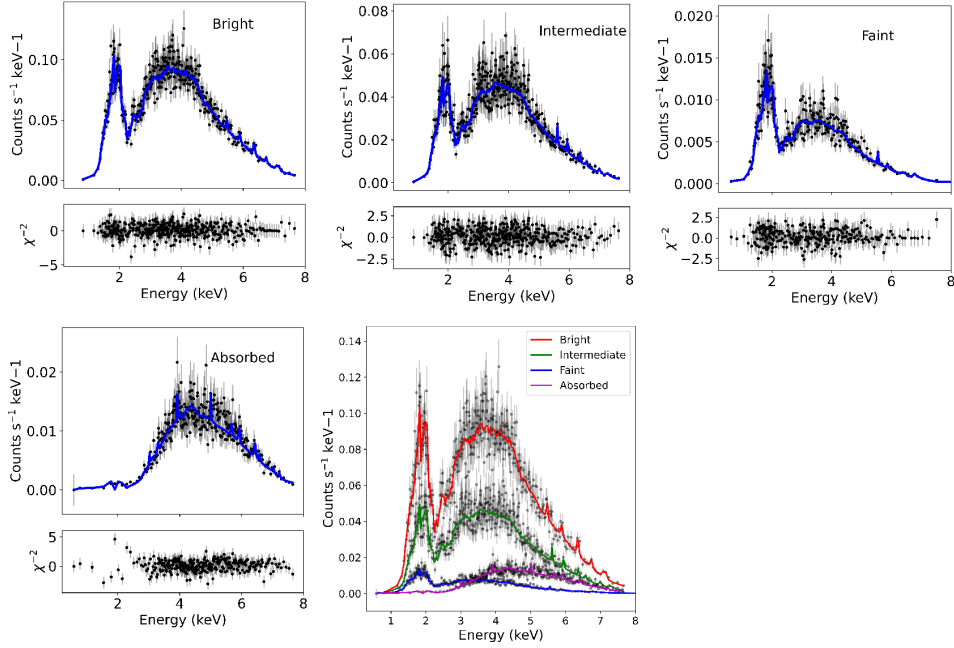


**Fig. B.2.** Upper row (left to right): Spectra, model, and  $\chi^2$  values for Bright, Intermediate and Faint. Lower row (left to right): Spectra, model, and  $\chi^2$  values for Absorbed and all spectra displayed for comparison.

## Appendix C: Emission lines present in all the spectra

**Table C.1.** Parameter values for the lines in the Bright, Intermediate, Faint, and Absorbed spectra.

Lines	Ce Center (keV)	Area (photons s <sup>-1</sup> cm <sup>-2</sup> )	EW (keV)	Cr Kα Center (keV)	Area (photons s <sup>-1</sup> cm <sup>-2</sup> )	EW (keV)	Fe Kα Center (keV)	Area (photons s <sup>-1</sup> cm <sup>-2</sup> )	EW (keV)	Fe Kα Center (keV)	Area (photons s <sup>-1</sup> cm <sup>-2</sup> )	EW (keV)	Fe Kβ Center (keV)	Area (photons s <sup>-1</sup> cm <sup>-2</sup> )	EW (keV)
Orb 1	5.60 <sup>+0.02</sup> <sub>-0.01</sub>	2.5 ± 2.3	7 ± 7	5.90 <sup>+0.03</sup> <sub>-0.02</sub>	2.5 ± 2.4	78 ± 8	6.400 <sup>+0.024</sup> <sub>-0.019</sub>	9 ± 4	30 ± 13	6.70 <sup>+0.13</sup> <sub>-0.16</sub>	4 ± 4	14 <sup>+15</sup> <sub>-14</sub>	7.0 <sup>+0.0</sup> <sub>-0.1</sub>	2 <sup>+5</sup> <sub>-2</sub>	8 <sup>+21</sup> <sub>-8</sub>
Orb 14	5.60 <sup>+0.03</sup> <sub>-0.11</sub>	0.4 <sup>+0.6</sup> <sub>-0.4</sub>	12 <sup>+19</sup> <sub>-12</sub>	6.00 <sup>+0.07</sup> <sub>-0.04</sub>	0.9 ± 0.7	12 ± 9	6.4 <sup>+0.1</sup> <sub>-0.0</sub>	0.3 <sup>+0.7</sup> <sub>-0.3</sub>	32 <sup>+70</sup> <sub>-30</sub>	6.60 <sup>+0.09</sup> <sub>-0.01</sub>	1.2 <sup>+1.0</sup> <sub>-0.9</sub>	13 <sup>+11</sup> <sub>-10</sub>	6.90 <sup>+0.07</sup> <sub>-0.06</sub>	1.4 <sup>+0.9</sup> <sub>-1.0</sub>	50 ± 40
Orb 31	5.60 ± 0.02	3.3 ± 2.0	22 ± 14	6.00 <sup>+0.03</sup> <sub>-0.04</sub>	4 ± 3	32 <sup>+22</sup> <sub>-21</sub>	6.40 <sup>+0.08</sup> <sub>-0.03</sub>	3 <sup>+4</sup> <sub>-2</sub>	30 ± 30	6.70 <sup>+0.11</sup> <sub>-0.02</sub>	7 ± 5	70 ± 50	6.90 <sup>+0.08</sup> <sub>-0.02</sub>	3 <sup>+4</sup> <sub>-2</sub>	30 <sup>+40</sup> <sub>-30</sub>
Orb 32	5.7 <sup>+0.0</sup> <sub>-0.2</sub>	1.7 <sup>+2.2</sup> <sub>-1.7</sub>	10 <sup>+13</sup> <sub>-10</sub>	5.90 <sup>+0.03</sup> <sub>-0.03</sub>	2.6 ± 2.4	16 ± 15	6.40 <sup>+0.03</sup> <sub>-0.03</sub>	4 ± 3	32 ± 20	6.6 <sup>+0.3</sup> <sub>-0.3</sub>	2 <sup>+3</sup> <sub>-2</sub>	17 <sup>+20</sup> <sub>-17</sub>	7.0 <sup>+0.0</sup> <sub>-0.1</sub>	3 ± 3	20 <sup>+30</sup> <sub>-20</sub>
Valley combined	5.5 <sup>+0.2</sup> <sub>-0.0</sub>	0.3 <sup>+0.7</sup> <sub>-0.3</sub>	20 <sup>+20</sup> <sub>-20</sub>	6.00 <sup>+0.08</sup> <sub>-0.02</sub>	1.1 ± 0.9	23 ± 17	6.40 <sup>+0.03</sup> <sub>-0.04</sub>	1.0 <sup>+1.2</sup> <sub>-0.9</sub>	20 <sup>+30</sup> <sub>-20</sub>	6.9 <sup>+0.9</sup> <sub>-0.3</sub>	1.0 <sup>+1.3</sup> <sub>-1.0</sub>	100 <sup>+130</sup> <sub>-100</sub>	7.00 <sup>+0.06</sup> <sub>-0.05</sub>	0.8 <sup>+1.4</sup> <sub>-0.8</sub>	90 <sup>+160</sup> <sub>-80</sub>
Bright	5.5 <sup>+0.1</sup> <sub>-0.0</sub>	5 ± 4	12 ± 9	5.90 <sup>+0.04</sup> <sub>-0.03</sub>	5 ± 4	12 ± 11	6.40 <sup>+0.06</sup> <sub>-0.01</sub>	11 ± 5	30 ± 15	6.70 ± 0.04	7 ± 6	23 ± 19	7.00 <sup>+0.04</sup> <sub>-0.06</sub>	1 <sup>+7</sup> <sub>-1</sub>	3 <sup>+30</sup> <sub>-3</sub>
Intermediate	5.60 ± 0.01	3 ± 2	16 ± 11	5.90 <sup>+0.06</sup> <sub>-0.02</sub>	2.6 ± 2.3	15 ± 13	6.4 ± 2.0	3 ± 3	19 ± 16	6.6 <sup>+0.3</sup> <sub>-0.0</sub>	3 ± 3	19 <sup>+22</sup> <sub>-19</sub>	7.00 ± 0.01	4 ± 4	30 ± 30
Faint	5.6 ± 2.0	0.6 ± 0.4	22 <sup>+17</sup> <sub>-19</sub>	5.90 <sup>+0.16</sup> <sub>-0.02</sub>	0.4 <sup>+0.5</sup> <sub>-0.4</sub>	19 <sup>+24</sup> <sub>-19</sub>	6.40 <sup>+0.03</sup> <sub>-0.07</sub>	0.8 ± 0.8	40 ± 40	6.80 <sup>+0.08</sup> <sub>-0.03</sub>	1.1 ± 0.9	70 ± 60	6.90 <sup>+0.08</sup> <sub>-0.02</sub>	1.3 <sup>+1.1</sup> <sub>-1.3</sub>	90 <sup>+80</sup> <sub>-90</sub>
Absorbed	5.7 <sup>+0.0</sup> <sub>-0.2</sub>	1.7 ± 1.7	13 ± 13	5.90 <sup>+0.09</sup> <sub>-0.03</sub>	2.3 ± 1.8	18 ± 15	6.40 <sup>+0.02</sup> <sub>-0.04</sub>	3.3 ± 2.2	30 ± 20	6.6 <sup>+0.3</sup> <sub>-0.0</sub>	1.7 <sup>+2.2</sup> <sub>-1.7</sub>	15 <sup>+19</sup> <sub>-15</sub>	7.0 <sup>+0.0</sup> <sub>-0.1</sub>	1.5 <sup>+2.3</sup> <sub>-1.5</sub>	14 <sup>+23</sup> <sub>-14</sub>

**Appendix D: Emission lines present Orb 32 and Absorbed spectra within the low energy spectra.****Table D.1.** Extra lines found in the Orb 32 and Absorbed spectra within the low energy spectra.

Line		Orb 32	Absorbed
Fe xvii	Center (keV)	$0.79^{+0.02}_{-0.01}$	$0.79^{+0.02}_{-0.0}$
	Area (photons s <sup>-1</sup> cm <sup>-2</sup> )	~ 64	~ 130
	EW (keV)	~ 140	-
Mg xi	Center (keV)	$1.40 \pm 0.03$	$1.40 \pm 0.04$
	Area (photons s <sup>-1</sup> cm <sup>-2</sup> )	$1.3^{+0.1}_{-0.8}$	$0.9^{+1.4}_{-0.7}$
	EW (keV)	$3100^{+100}_{-1900}$	$300^{+500}_{-200}$
Fe xxiv	Center (keV)	$1.50^{+0.01}_{-0.02}$	$1.50^{+0.03}_{-0.02}$
	Area (photons s <sup>-1</sup> cm <sup>-2</sup> )	$0.5^{+0.0}_{-0.3}$	$0.4^{+0.0}_{-0.3}$
	EW (keV)	$8000^{+300}_{-5000}$	$1900^{+10}_{-1400}$
Mg xii	Center (keV)	$1.70^{+0.00}_{-0.01}$	$1.70^{+0.01}_{-0.02}$
	Area (photons s <sup>-1</sup> cm <sup>-2</sup> )	$0.5^{+0.7}_{-0.2}$	$0.4^{+0.8}_{-0.2}$
	EW (keV)	$6000^{+9000}_{-3000}$	$50000^{+90000}_{-30000}$
Si xiii	Center (keV)	$1.90 \pm 0.01$	$1.90 \pm 0.02$
	Area (photons s <sup>-1</sup> cm <sup>-2</sup> )	$0.7^{+0.7}_{-0.3}$	$0.7^{+0.8}_{-0.3}$
	EW (keV)	$3000^{+3000}_{-1000}$	$12000^{+15000}_{-5000}$
Si xiv	Center (keV)	$2.00 \pm 0.01$	$2.00^{+0.01}_{-0.07}$
	Area (photons s <sup>-1</sup> cm <sup>-2</sup> )	$0.4^{+0.4}_{-0.2}$	$0.4^{+0.1}_{-0.3}$
	EW (keV)	$2200^{+2400}_{-1200}$	$170^{+30}_{-130}$
Si xiii	Center (keV)	$2.10 \pm 0.03$	$2.10 \pm 0.02$
	Area (photons s <sup>-1</sup> cm <sup>-2</sup> )	$0.6^{+0.6}_{-0.4}$	$0.9^{+0.6}_{-0.5}$
	EW (keV)	$400^{+300}_{-400}$	$1100^{+10}_{-1100}$
Mg xii	Center (keV)	$2.00^{+0.03}_{-0.02}$	$2.00^{+0.01}_{-0.02}$
	Area (photons s <sup>-1</sup> cm <sup>-2</sup> )	$0.3^{+0.3}_{-0.2}$	$0.4^{+0.6}_{-0.3}$
	EW (keV)	~ 700	$300^{+40}_{-300}$

**Appendix E: Emission lines present Orb 32 and Absorbed spectra within the high energy spectra.****Table E.1.** Extra lines found in the Orb 32 and Absorbed spectra in the high energy spectra.

Orb 32		Absorbed	
S xv	Center (keV)	$3.00^{+0.18}_{-0.02}$	$3.00^{+0.07}_{-0.04}$
	Area (photons s <sup>-1</sup> cm <sup>-2</sup> )	$3^{+7}_{-3}$	$2^{+3}_{-2}$
	EW (keV)	$10^{+300}_{-10}$	$14^{+11}_{-14}$
Ar xviii	Center (keV)	$3.3^{+0.0}_{-0.2}$	$3.3^{+0.0}_{-0.2}$
	Area (photons s <sup>-1</sup> cm <sup>-2</sup> )	$2^{+5}_{-2}$	$2.0^{+2.4}_{-2.0}$
	EW (keV)	$\sim 12$	$\sim 10$
Ca xix	Center (keV)	$3.90 \pm 0.01$	$3.90^{+0.07}_{-0.03}$
	Area (photons s <sup>-1</sup> cm <sup>-2</sup> )	$3.6^{+2.3}_{-2.2}$	$1.9 \pm 1.5$
	EW (keV)	$10^{+2400}_{-10}$	$20^{+30}_{-20}$
Ca xx	Center (keV)	$5.10^{+0.00}_{-0.02}$	$5.00 \pm 0.01$
	Area (photons s <sup>-1</sup> cm <sup>-2</sup> )	$1.6 \pm 1.6$	$1.3 \pm 1.2$
	EW (keV)	$9^{+100}_{-9}$	$9^{+500}_{-9}$